



Comparative Molecular Field Analysis of Selective A₃ Adenosine Receptor Agonists

Suhaib M. Siddiqi,^a Robert A. Pearlstein,^b Lawrence H. Sanders^a and Kenneth A. Jacobson^{a*}

^a*Molecular Recognition Section, Laboratory of Bioorganic Chemistry, National Institute of Diabetes, Digestive and Kidney Diseases, National Institutes of Health, Bethesda, MD 20892, U.S.A.*

^b*Division of Computer Research and Technology, National Institutes of Health, Bethesda, MD 20892, U.S.A.*

Abstract—A series of 48 *N*⁶-benzyladenosine 5'-uronamide derivatives has been described recently as moderately selective A₃ adenosine receptor agonists of nanomolar potency (Gallo-Rodriguez, C. *et al. J. Med. Chem.* **1994**, *37*, 636). Quantitative structure activity relationships in this series, including some novel derivatives, have been investigated using a Comparative Molecular Field Analysis (CoMFA), with emphasis on the *N*⁶-substituent. The resulting three dimensional pharmacophore model defines the steric and electronic factors which modulate *in vitro* affinities in binding to rat brain A₃ adenosine receptors. The model indicates a positive correlation of affinity with the steric characteristics of the compounds (major factor), particularly toward the 3-position of the benzyl ring of *N*⁶-benzyl NECA, and a weak correlation with the electrostatic effects of the *N*⁶-substituent. A comparison of active and inactive compounds using volume maps showed that bulk at the 3-position of the benzyl ring of the molecule is conducive to high affinity at A₃ receptors, while steric bulk at other positions of the benzyl ring leads to poor binding. *t*-Boc-amino acid conjugates of a 3-aminobenzyl derivative were synthesized to probe the steric and hydrophobic limitations at that position. We have discovered a subregion of the *N*⁶-benzyl binding pocket occupied by a 3-(*L*-prolylamino) group that is sterically disallowed at A₃ receptors and allowed in A₁ and A_{2a} receptors. 6-*N*-Phenylhydrazino and 6-*O*-phenylhydroxylamino derivatives, incorporating major changes in electrostatic character of the ligand proximal to the purine, were predicted by the CoMFA model to have high A₃ affinity. Such analogs were synthesized and found to be well tolerated at the A₃ receptor binding site.

Introduction

The structural requirements for purines as ligands at A₁ and A₂ adenosine receptors have been explored in detail.^{1–3} Recently, a novel rat A₃ adenosine receptor subtype was discovered through the cloning of cDNA coding for sequences resembling G-protein-coupled receptors.⁴ The rat A₃ receptor showed only 56% sequence homology with the rat A₁ receptor, and was also distinct in pharmacological properties, e.g. the classical A₁ and A₂ antagonists such as alkylxanthines do not bind to rat A₃ receptors. The three-dimensional structure of the rat A₃ receptor was modeled⁵ by analogy to bacteriorhodopsin. Activation of A₃ receptors has characteristic biological effects, such as enhancement of the release of inflammatory mediators from a rat mast cell line,^{6,7} hypotension,⁸ and depression of locomotor activity.⁹ Chronic administration of an A₃ agonist has a cerebro-

protective effect in a stroke model in gerbils, thus there is considerable potential for development of therapeutic agents acting at this receptor.¹⁰ The activation of A₃ receptors is also suggested to be at least partially responsible for the protective preconditioning of the ischemic heart by prior exposure to adenosine agonists.¹¹

The structure–activity relationships (SAR) for adenosine and xanthine derivatives at rat A₃ receptors have been reported.^{5,12} Highly selective agonists have recently been synthesized.^{12,13} The combination of *N*⁶-benzyl- and 5'-*N*-alkyluronamide modifications of adenosine favored increased A₃ receptor binding affinity and selectivity versus A₁ and A_{2a} receptors.⁵ Optimization of substituents at the *N*⁶-benzyl position produced a highly potent A₃ agonist, *N*⁶-(3-iodobenzyl)-adenosine-5'-*N*-methyluronamide (IB-MECA, Fig. 1), which is 50-fold selective in binding assays for rat A₃ versus either A₁ or A_{2a} receptors.¹² Further modification indicated that 2-substitution, such as chloro, methylamino or methylthio, in combination with the IB-MECA structure enhanced A₃ selectivity.

Comparative molecular field analysis (CoMFA)^{14,15} is a promising technique for studying quantitative structure activity relationships (QSAR). Based on both physical and biological properties with a homologous series, CoMFA defines the relative contributions of three-dimensional steric and electrostatic fields towards the potency. Such an approach appeared to be suited to study the binding

Abbreviations: [¹²⁵I]AB-MECA, *N*⁶-(4-amino-3-iodobenzyl)-adenosine-5'-*N*-methyluronamide; Boc, *tert*-butoxycarbonyl; CGS 21680, 2-[4-[(2-carboxyethyl)phenyl]-ethyl-amino]-5'-*N*-ethylcarboxamidoadenosine; CoMFA, comparative molecular field analysis; DMF, *N,N*-dimethylformamide; DMSO, dimethylsulfoxide; EDAC, 1-(3-dimethylaminopropyl)-3-ethylcarbodiimide hydrochloride; IB-MECA, *N*⁶-(3-iodobenzyl)-adenosine-5'-*N*-methyluronamide; NECA, 5'-*N*-ethylcarboxamidoadenosine; PIA, *R,N*⁶-phenylisopropyladenosine; PLS, partial least squares; QSAR, quantitative structure activity relationship; rms, root mean square; Tris, tris(hydroxymethyl)aminomethane.

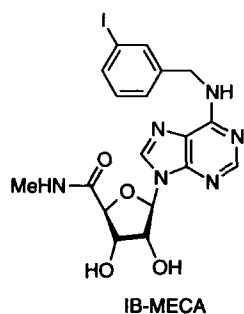


Figure 1.

affinities of this series of A_3 -selective agonists (N^6 -benzyladenosine-5'- N -alkyluronamides), since numerous analogs close in structure and their K_i values in radioligand binding have been reported. In general, results of QSAR analysis for a specific set of compounds may lead to an understanding of the mechanism of molecular recognition, and ideally have predictive capabilities for the design of more selective agents. A quantitative structure-activity model of the A_3 pharmacophore would aid in the design of more selective agonists and perhaps indicate a

means of designing antagonists. In this study we use CoMFA to model various N^6 -benzyladenosine-5'-uronamides including some novel derivatives, with emphasis on the N^6 -substituent, since that is the site of most of the structural modifications reported. The binding data used in the CoMFA model were previously reported by our laboratory¹² or determined in this study for newly synthesized adenosine derivatives.

Chemistry

The synthesis of compounds **12–53** in Tables 1 and 2 was reported previously.¹² The synthesis of agonist analogs **5**, **6**, **7**, **10**, and **11** is shown in Schemes 1 and 2. The intermediate 2',3'-isopropylidene-6-chloropurine-5'-methyluronamide (**1**)¹² was heated with 3-aminobenzylamine to yield compound **2**. The aryl amino derivative **2** was then condensed with several *t*-butoxycarbonyl (*t*-Boc) amino acids, e.g. *t*-Boc-L-proline or *t*-Boc- β -alanine, using 1-(3-dimethylaminopropyl)-3-ethylcarbodiimide hydrochloride (EDAC) in the presence of 4-(N,N -dimethylamino)-

Table 1. Affinities of 5'-uronamide derivatives in radioligand binding assays at rat brain A_1 , A_2 , and A_3 receptors^{a,c}

K_i (nM) or % inhibition

Compound	R_1	R_2	$pK_i(A_3)^c$	Predicted ^f pK_i
12 ^d	H	NH ₂	5.85	5.92
13 ^d	Me	NH ₂	7.14	7.31
14 ^d	Et	NH ₂	6.95	7.02
15 ^d	cyclopropyl	NH ₂	5.80	5.92
16	H ₂ NEt-	NH ₂	4.83	4.80
17	BocNHEt-	NH ₂	4.74	4.76
18	Me	OH ^e	5.21	5.34 (4.98) ^h
19 ^e	Et	OH ^e	5.3	5.46 (5.13) ^h

^aDisplacement of specific [³H]PIA binding, unless noted, in rat brain membranes expressed as $K_i \pm$ SEM in nM ($n = 3$).

^bDisplacement of specific [³H]CGS 21680 binding, unless noted, in rat striatal membranes, expressed as $K_i \pm$ SEM in nM ($n = 3$).

^cDisplacement of specific binding of [¹²⁵I]APNEA¹⁸ or [¹²⁵I]4-amino-3-iodobenzyladenosine-5'- N -methyluronamide³⁰ from membranes of CHO cells stably transfected with the rat A_3 -cDNA, expressed as $K_i \pm$ SEM in nM ($n = 3-5$).

^dValues at A_1 and A_2 receptors are taken from Bruns *et al.*³¹ K_i values at A_1 receptors are versus specific binding of [³H]W⁶-cyclohexyladenosine. K_i values at A_2 receptors are versus specific binding of [³H]NECA in the presence of 50 nM CPA in rat striatal membranes.

^eValues from van Galen *et al.*³

^fPredicted 'within' the model by cross-validation during derivation.

^gModeled as hydroxy tautomers because of the similarity of OH to NH.

^hPredicted pK_i for keto tautomer.

Table 2. Affinities of *N*⁶-benzyladenosine 5'-uronamide derivatives in radioligand binding assays at rat brain A₁, A₂, and A₃ receptors^{a-c}

R₄ = H, unless noted
X = H, unless noted

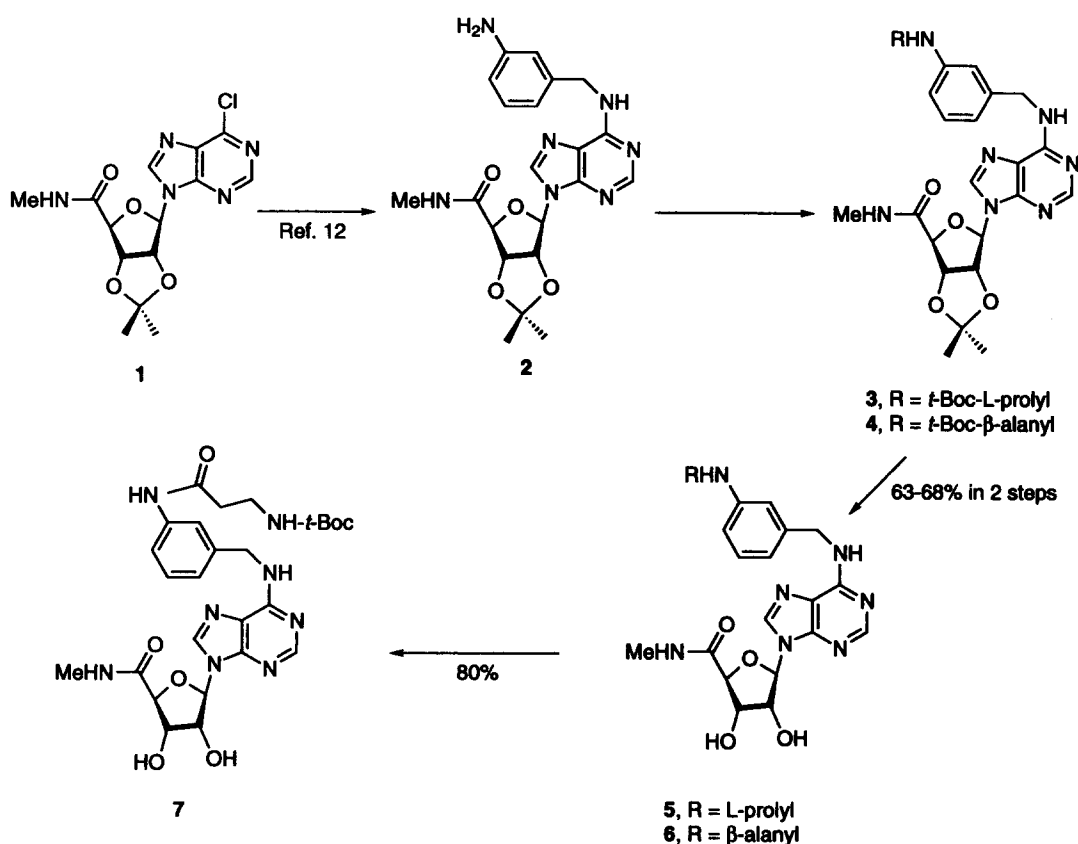
Compound	R ₁	R ₅	pK _i (A ₃) ^c	Predicted ^d pK _i
20	H	H	6.61	6.68
21	Me	H	7.80	7.91
22	Me	3-Cl	7.66	7.88
23	Me	3-Br	8.72	8.63
24	Me	3-I	8.96	9.20
25	Me	3-NO ₂	7.72	7.80
26	Me	3-NH ₂	7.55	7.68
27	Me	3-NHCOCH ₃	7.38	7.52
28	Me	3-CH ₃	8.00	8.21
29	Me	3-CF ₃	7.51	7.58
30	Me	4-Cl	7.77	7.80
31	Me	4-Br	7.92	8.00
32	Me	4-NH ₂	7.85	7.83
33	Me	4-NH ₂ , 3-I	8.91	8.30
34	Et	H	8.17	8.35
35	Et	H (R-, R ₄ = CH ₃)	7.74	7.79
36	Et	H (S-, R ₄ = CH ₃)	6.31	6.51
37	Et	3-F	7.97	7.93
38	Et	3-Cl	8.96	8.87
39	Et	3-Br	8.55	8.35
40	Et	3-I	9.05	8.88
41	Et	2-NO ₂	8.55	8.50
42	Et	3-NO ₂	8.06	8.30
43	Et	4-NO ₂	8.04	8.51
44	Et	3-CH ₃	8.92	8.45
45	Et	2-OMe	8.15	8.20
46	Et	3-OMe	8.37	8.40
47	Et	4-OMe	7.96	7.82
48	cyclopropyl	H	6.99	7.00
49	Me	I	9.48	9.40
		X = Cl		
50	Me	I	8.64	8.60
		X = SMe		
51	Me	I	8.51	8.49
		X = NHMe		

^aDisplacement of specific [³H]PIA binding, unless noted, in rat brain membranes expressed as K_i ± SEM in nM (n = 3–6).

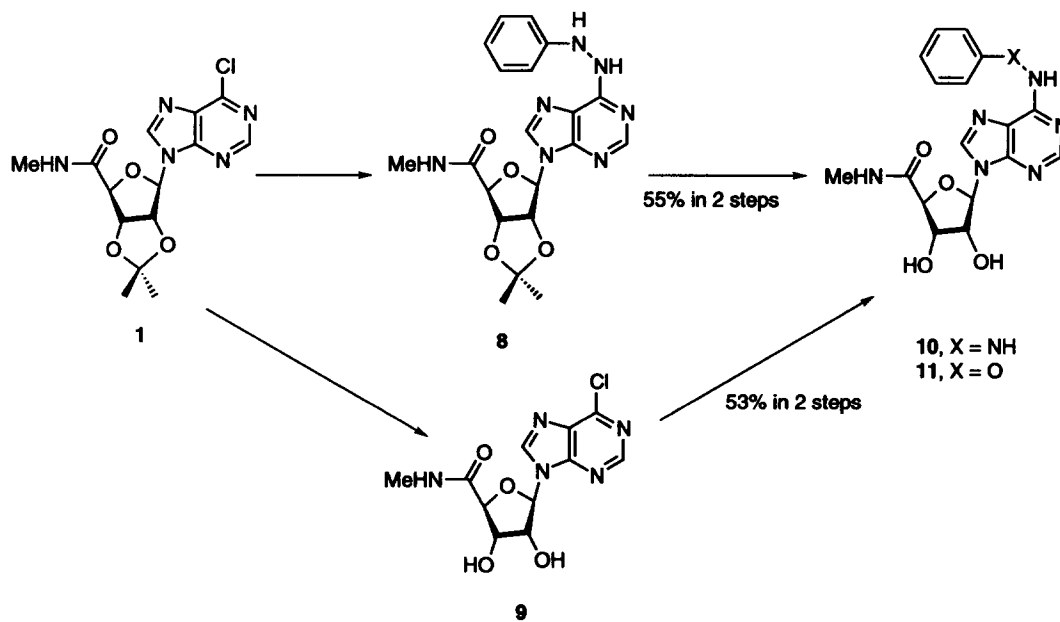
^bDisplacement of specific [³H]CGS 21680 binding, unless noted, in rat striatal membranes, expressed as K_i ± SEM in nM (n = 3–6).

^cDisplacement of specific binding of [¹²⁵I]APNEA¹⁸ or [¹²⁵I]4-amino-3-iodobenzyladenosine-5'-N-methyluronamide³⁰ from membranes of CHO cells stably transfected with the rat A₃-cDNA, expressed as K_i ± SEM in nM (n = 3–5).

^dPredicted 'within' the model by cross-validation during derivation.



Scheme 1.



Scheme 2.

pyridine and imidazole provided compounds 3 and 4, respectively. Following deprotection of both isopropylidene and *t*-Boc groups by treatment with acid, the corresponding amines, compounds 5 and 6, were obtained. Compound 6 was then acylated with di-*tert*-butyldi-carbonate to give the *t*-Boc derivative 7.

To investigate the relative influence of electronic and steric factors as predicted by the CoMFA model (see below) the methylene group of the *N*⁶-benzyl substituent was modified with heteroatoms. Thus, *N*⁶-NH-O- and -NH-NH- analogs, 10 and 11, respectively, were synthesized (Scheme 2). The synthesis began with the

displacement of the 6-chloropurine riboside derivative, compound **1**, upon heating with phenylhydrazine to provide compound **8**. Compound **8** was then deprotected under acidic conditions to provide the hydrazine derivative, compound **10**. The corresponding reaction of **1** with *O*-phenylhydroxylamine was unsuccessful, but the desired product, compound **11**, could be obtained by first deprotecting the isopropylidene group of **1** followed by displacement.

Receptor Binding

Newly synthesized adenosine analogs were tested in radioligand binding assays for affinity at rat brain A₁, A₂ and A₃ adenosine receptors. A₃ receptor affinity was measured in Chinese hamster ovary (CHO) cells, stably expressing cloned rat brain A₃ receptors.⁴⁵ These cells were provided by Professor Gary Stiles and Dr Mark Olah of Duke University Medical Center. The radioligand used for binding to A₃ receptors was [¹²⁵I]AB-MECA (4-amino-3-iodobenzyladenosine-5'-*N*-methyluronamide).¹⁶ Affinity at A₁ receptors was measured in rat cortical membranes using [³H]*N*⁶-*R*-phenylisopropyladenosine¹⁷ and at A₂ affinity in rat striatal membranes using [³H]CGS 21680, as reported.¹⁸

Computational Methods

Materials and approaches

CoMFA provides steric and electrostatic field representations of ligand molecules, field fitting to optimize mutual alignment within a series of molecules, cross-validation¹⁵ to indicate the predictive validity of the correlations, and graphic representation of the results. The molecular modeling and CoMFA studies were performed on a Silicon Graphics IRIS Indigo R4000XZ workstation running SYBYL 6.04.¹⁹ MOPAC (version 6.0)²⁰ and AM1 parameter sets^{21,22} were used for calculating partial atomic charges and full energy minimization of the ligands (keywords: PREC, GNORM = 0.1, MMOK, EF). CoMFA was used as a three-dimensional QSAR method to analyze the correlations between the measured binding affinities and the steric and electrostatic properties of the ligand molecules, as evaluated by a positive probe atom. Cross-validation evaluates a model by how well it predicts rather than fits the data, therefore cross-validation is an important criterion for CoMFA models. Partial least squares (PLS) regression analysis²³ on the training set of 37 compounds (Tables 1 and 2) was carried out on a subset of steric and electrostatic energy having a standard deviation ≤ 1.0 kcal mol⁻¹. The steric and electrostatic fields were subjected to scaling in order to assign them the same weight (the command 'scaling CoMFA_std' was used). Cross-validation procedure¹⁵ was carried out by dividing the training set into 10 randomly selected groups. The optimal number of latent variables was that of the cross-validation equation, with the lowest standard error and significance level estimated by means of the stepwise *F*-test to be $\geq 99.5\%$. Bootstrap analysis¹⁵ of the dataset

provided a means by which statistical confidence limits could be placed on the results. Three-dimensional contour plots can be used to display the CoMFA results graphically and to generate ideas for designing novel agonists. After being subjected to field probing, the biological activities of these untested structures may then be quantitatively predicted, ideally within statistical confidence limits. The compound structures and biological activity data used to construct QSAR analyses reported herein are found in Tables 1 (5'-uronamide modifications) and 2 (*N*⁶-benzyl modifications).

Molecular models and the alignment rules

Attempts to obtain crystals of sufficiently good quality of *N*⁶-benzyladenosine 5'-uronamide derivatives, for X-ray purpose, were unsuccessful, therefore the Cambridge Structural Database (CSD) was searched for *N*⁶-(3- or 4-substituted benzyl)-adenosine derivatives. The crystal coordinates for *N*⁶-(4-nitrobenzyl)-2'-deoxyadenosine were retrieved from the CSD. This structure was modified to *N*⁶-(3-iodobenzyl)-5'-methyluronamide (IB-MECA, **24**), hydrogen atoms were added, and it was fully geometry optimized using the standard TRIPOS molecular mechanics force field with a 0.001 kcal mol⁻¹ energy gradient convergence criterion and a distance-dependent dielectric. Partial atomic charges were determined using MOPAC calculations.²²

SYBYL and MOPAC were used to calculate the conformational properties of IB-MECA. The three bonds of purine-NH-CH₂-Ph (Table 3) were searched at 30° increments using the systematic search option of SYBYL. This resulted in 658 possible conformers, which were fully energy minimized using the TRIPOS molecular mechanics force field. Eighty-one minimum energy conformers having energies in the range of -25.18 to -27.80 kcal mol⁻¹ were found. Each of these conformers was then fully energy minimized using MOPAC. The above process led to four families of conformers: family A contained 37 conformers, family B contained six conformers, family C contains 28 conformers, and family D contained 10 conformers. The typical dihedral angle values defining the four families are reported in Table 3. In order to investigate conformational effects of 5'-*N*-alkyl carboxamido group on the *N*⁶-benzyl moiety, a conformational search of the carboxamido group of compound **40**, from family A (Table 2), was performed. The three bonds C4'-C5'-N5'-C were searched at 30° increments using the systematic search option of SYBYL, which resulted in 105 conformers. Each of the resulting conformers was fully energy minimized using TRIPOS molecular mechanics force field. Since the contributions of modifications at *N*⁶- and 5'-substituted adenosine towards A₃ potency were found empirically to be additive and not interdependent,^{5,12,13} the conformations of the *N*⁶-benzyl and 5'-carboxamido groups were treated independently in this study. Therefore, conformational properties of C5'-carboxamido groups could be fixed while studying details of the *N*⁶-benzyl group. In order to evaluate which of the above mentioned four families will produce a data set with the highest confidence limit (see discussion of the CoMFA

r^2 parameter below), one typical conformer was selected as a representative of each family. Each of these conformers was modified to the individual ligand structure (compounds 24–29, 32, 33, 41, and 45) using the editing tools in SYBYL. Each structure was fully geometrically optimized using MOPAC, and the resulting partial atomic charges were used in the CoMFA calculations. Compounds 24–29, 32, 33, 41, and 45 were aligned to IB-MECA (24), a potent A_3 receptor agonist, by field-fit minimization techniques, and four data sets were created for each conformer family. Since family A gave the highest confidence limit (Table 3), the CoMFA data set, containing all the ligands from Tables 1 and 2, was built based upon this conformation. It is noteworthy to mention that van Galen and co-workers²⁴ proposed that the N^6 -substituted high-affinity ligands for adenosine receptors have a preferred $N1-C6-N^6-C^2$ torsion angle of -75° . Family A, from the conformational search, has a torsion angle of -75° for $N1-C6-N^6-C^2$ bonds. All fully geometry optimized structures, using MOPAC, had an envelope-like conformation at $C2'$ and $C3'$ position and showed a torsion angle of 69.8° for $O4'-C1'-N9-C8$ bond (9 β -glycosyl bond).

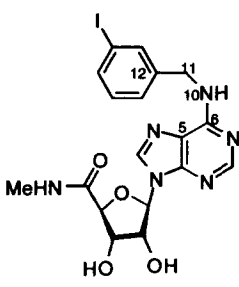
The positioning of a molecular model relative to a template within a fixed lattice is the most important variable in CoMFA, because interaction energies depend strongly on relative molecular positions. The field-fit procedure is one of the alignment rules which can be used to increase field similarity within a series of molecules.¹⁴ IB-MECA was chosen as the template molecule on which to align the various A_3 receptor ligands and to test new structures. They were aligned via root mean square (rms) fit of their purine ring carbons to the corresponding carbons of the IB-MECA template molecule. The cross-validated and non-cross-validated PLS analyses on the training set of 37 compounds (Tables 1 and 3) based on this alignment scheme gave a CoMFA data set of less

reliability in terms of r^2 . A second CoMFA data set, containing all the 37 ligands from Tables 1 and 3, was created by rms fit of the purine ring carbons to the corresponding carbons of the IB-MECA template molecule, followed by field-fit optimization of each ligand to the template molecule, in order to obtain maximal similarity between the steric and electrostatic fields of template and test molecules. Field-fit optimization forced the aligned molecules into initially high energy conformations which caused changes in the conformation and energy of the ligands compared to the original MOPAC-minimized conformations of the ligands. Therefore, subsequent molecular mechanics re-minimization without the field-fit option allowed the fitted molecules to relax to the nearest local minimum energy structure. This alignment scheme was chosen for CoMFA calculations because it provided the most direct comparison of substituent effects and yielded the most predictive model.

CoMFA: interaction energy calculations and regression techniques

In CoMFA the single molecule under inspection is presented in a grid box, in which user-defined atoms rest at the grid points interacting with the proximal structure. The physical chemistry of these interaction processes is described by an approximation in terms of classical mechanics. In our model, the steric field, defined in terms of the van der Waals (Lennard-Jones 6–12) interactions, and the electrostatic field (based on a Coulombic term having a $1/r$ distance-dependent dielectric) were calculated using an sp^3 carbon probe atom (with a charge of +1 and a van der Waals radius of 1.52 Å) on a regularly-spaced three-dimensional lattice. The dimensions of CoMFA lattice were determined through an automatic procedure, featured by the SYBYL/CoMFA routine, which extends the lattice walls beyond the dimensions of each structure

Table 3. Average dihedral angles and correlation coefficient of four IB-MECA conformer families



$\Psi_2 \backslash \Psi_1$ (degrees)	+80	+170
+25	Family D (~12%) ($r^2 = 0.19$) ^a	Family C (~35%) ($r^2 = 0.16$) ^a
-170	Family A (~45%) ($r^2 = 0.42$) ^a	Family B (~8%) ($r^2 = 0.36$) ^a

$$\Psi_1 = C_6 - N_{10} - C_{11} - C_{12}$$

$$\Psi_2 = C_5 - C_6 - N_{10} - C_{11}$$

^aThese non-cross-validated r^2 values were measured on the test data sets of compounds 24–29, 32, 33, 41, and 45.

by 4.0 Å in all directions. The lattice spacing was set to a value of 2.0 Å. This automatically generated lattice contained 720 points. The steric and electrostatic energy values were truncated to 30 kcal mol⁻¹; the electrostatic ones were not dropped in correspondence of lattice points inside the union volume of the superimposed ligands.

Initial PLS analyses were performed in conjunction with the cross-validation (leave-one-out method) option to obtain the optimal number of components to be used in the subsequent analyses of the dataset. The PLS analysis was repeated with the number of cross-validation groups set to zero. The optimal number of components was designated as that which yielded the highest cross-validated r^2 values in the non-cross-validated (conventional) analyses. The final PLS analysis with 10 bootstrap groups and the optimal number of components was performed on the dataset.

After the optimal dimensionality of each model was established, by PLS analysis and cross-validation procedure, the corresponding calibration equation (resulting from the simultaneous contribution of all the observations) was derived. The calibration equation with latent variables was then converted to the original parametric space represented by probe–ligand interaction energies; a 3-D-QSAR was therefore derived whose coefficients were associated with statistically significant lattice locations. CoMFA coefficient contour maps were generated by interpolation of the pairwise products between the 3-D-QSAR coefficients and the standard deviations of the associated energy variables. The derived 3-D-QSAR calibration model was successively employed

to forecast the binding affinity values of the five compounds listed in Table 4.

'Predictive' r^2 values

The 'predictive' r^2 was based only on molecules not included in the training set and is defined as explained by Marshall and coworkers.²⁵

Results

CoMFA of A₃ receptor binding affinity

Structural changes in a series of ligands sometimes may cause also electronic changes of substituents which are supposed to be invariant in the series. In organic chemistry this effect is termed 'reversion of polarity'. For these cases one needs a higher level of electronic description, e.g. charge calculation or estimation of electron density by at least semiempirical methods. In our CoMFA training set the important structural transition is substituent variation in the aromatic moiety at the N⁶-position. Therefore, partial atomic charges were calculated by AM1 parameter sets. The results of the CoMFA are summarized in Table 5. The partial least square (PLS) algorithm was used in conjunction with the cross-validation option to obtain the optimal number of components to be used in the subsequent analyses of the dataset. The PLS analysis based on field-fit alignment gave a correlation with a cross-validated r^2 of 0.631 with the maximum number of components set equal to five (maximum number of components set equal to 3, 6, 7 or 8 gave unreliable cross-

Table 4. Affinities of the new N⁶-benzyladenosine 5'-uronamide derivatives in radioligand binding assays at rat brain A₁, A₂, and A₃ receptors^{a,c}

X = CH₂ unless noted
K_i (nM)

compd	R	pK _i (A ₃) ^c	K _i (A ₁) ^a	K _i (A ₂) ^b	Predicted pK _i (A ₃) ^d	A ₁ /A ₃	A ₂ /A ₃
5	L-prolyl-NH	4.93	170 ± 30	215 ± 54	8.11	0.014	0.018
6	β-alanyl-NH	7.64	101 ± 9	144 ± 40	7.56	4.5	6.3
7	t-Boc-β-alanyl-NH	7.33	4500 ± 1050	1960 ± 410	7.41	96	42
10	R = H, X = NH	6.65	3940 ± 240	7160 ± 80	6.86	18	31
11	R = H, X = O	5.87	2060 ± 370	66300 ± 16200	5.86	50	2

^aDisplacement of specific [³H]PIA binding, unless noted, in rat brain membranes expressed as K_i ± SEM in nM (n = 3).

^bDisplacement of specific [³H]CGS 21680 binding, unless noted, in rat striatal membranes, expressed as K_i ± SEM in nM (n = 3).

^cDisplacement of specific binding of [¹²⁵I]APNEA¹⁸ or [¹²⁵I]4-amino-3-iodobenzyladenosine-5'-N-methyluronamide³⁰ from membranes of CHO cells stably transfected with the rat A₃-cDNA, expressed as K_i ± SEM in nM (n = 3–5). The K_i (A₃) for 5 = 11,800 ± 1400, 6 = 22.7 ± 8.2, 7 = 46.7 ± 15.1, 10 = 225 ± 29, 11 = 1340 ± 230.

^dPredicted by the model without being included in the trial dataset.

validated r^2 ; $r^2 \geq 0.40$) and the cross-validation groups set equal to the number of observations (rows) in the data table. The non-cross-validated analysis was repeated with the optimum number of components, as determined by the cross-validated analysis, to give an r^2 of 0.798. In order to obtain statistical confidence limits, the non-cross-validation analysis was repeated with 10 bootstrap groups, which yielded an $r^2 = 0.897$ (optimum number of components was 5), $\text{sep} = 0.556$, $s = 0.146$, $F_{\text{test}} = 64.538$, $p = 0.000$, steric contribution = 0.847 and electrostatic contributions = 0.153. These parameters are explained in Table 5.

The CoMFA-derived QSAR of the A_3 ligands exhibited a strong cross-validated correlation, indicating that it was highly predictive. Cross-validation provides information concerning the predictive ability of the QSAR dataset by minimizing the occurrence of chance correlations in the QSAR model. A small difference between cross-validated and non-cross-validated r^2 values is indicative of reliable correlations in the QSAR dataset. The relatively small difference between cross-validated and conventional r^2 values here indicated only a minor influence of spurious correlations in the datatable. The bootstrapped r^2 value was very high with a small standard deviation, thus indicating a high degree of confidence in the analysis. The predicted binding affinities obtained from the analysis are plotted versus the actual values in Figure 2.

The CoMFA steric and electrostatic fields for the analysis are presented as three-dimensional color-coded contour plots in Figures 3 and 4. In Figure 3 the green polyhedra represent areas in space around the molecules where steric bulk correlates with increased binding affinity. The field values are calculated as the scalar product of the β -coefficient and the standard deviation associated with a particular column in the QSAR table ($\text{stdev} \times \text{coeff}$). The values corresponding to steric columns are plotted as the percentage of contribution to the QSAR equation. It is necessary to point out that the 3 and 5 positions of N^6 -benzyl group were mixed during the alignments for different compounds to test if steric hindrance can be tolerated at both positions. Of particular interest are the green polyhedra around the 3-position (equivalent to 5-position) of the N^6 -benzyl substituent, the yellow polyhedron around the 4-position of the N^6 -benzyl substituent, and the N^6 -CH₂- group. The blue polyhedra

around the N^6 -CH₂- group suggest a tolerance for the positive charge. Our previous SAR studies indicated that some substitution at the 3-position of the N^6 -benzyl group increased the binding affinity of the agonists, while substitution at the 4-position of N^6 -benzyl and N^6 -CH₂-groups reduced the binding affinity.²⁶ Clearly, the phenylhydrazine derivative **10** (Table 4), which would increase the positive charge in that region, by the possible protonation of nitrogen atoms, showed a selectivity for A_3 versus A_{2A} receptors comparable to that of the carbon analog, N^6 -benzyladenosine-5'-methyluronamide (**21**). It is interesting to note that in Figure 4 the area of disfavored positive charge (90% contribution) at the 3-position, designated by blue polyhedra, overlaps the area previously defined as being tolerant to increases in steric bulk (Fig. 3). This indicates that this area of the binding site may show a preference for bulky electronegative group, such as the iodo group of the potent A_3 adenosine receptor agonist IB-MECA, **24**. We were interested to explore further tolerance for hydrophobic interactions at the 3-position of the N^6 -benzyl moiety. Therefore, we synthesized the *t*-Boc-alanyl conjugate, (**7**), and the A_3 binding affinity of **7** ($K_i = 47$ nM) suggested that a bulky hydrophobic group is tolerated at this position. The newly synthesized molecules **5–7** extended 3.38 Å in the space occupied by the derived model. The fact that four out of five new molecules were well predicted offers information on predictability of our CoMFA model.

The contour plot for positive steric contribution (green) shown in Figure 3 emphasizes the importance of a proper substitution on the N^6 -benzyl group of 5'-uronamide derivatives for maximizing receptor binding, whereas the contour plot of negative steric contribution (Fig. 3) emphasizes the importance of sterically unfavored substitutions in binding affinity. These plots, indicating the importance (or lack thereof) of substitutions, such as iodide which enhances affinity, in various positions on an adenosine N^6 -benzyl moiety using a simple plus/minus notation, are qualitatively similar to a previous representation of HIV-inhibitors by Safe.²⁷ The appropriateness of the alignment used is supported by the success achieved with the QSAR for the binding data for the β -alanyl conjugates, compounds **6** and **7**. It should be pointed out that CoMFA contour maps are not directly comparable to receptor maps. In fact, the major contribution of electronegative substituents at the 3-

Table 5. CoMFA QSAR results of A_3 ligands

Alignment Rule	$r^2_{\text{cross}}^b$	r^2	sep^c	F_{test}^d	p value	$r^2_{\text{bs}}^e$	Steric contribution	Electrostatic contribution	Std Dev. ^f
rms Multifit	0.40	0.746 (5) ^a	0.684	41.132	0.000	0.802	0.924	0.076	0.036
Field-Fit	0.631	0.798 (5) ^a	0.556	64.538	0.000	0.897	0.847	0.153	0.017

^aNumbers in parentheses are optimal number of components.

^bCross-validated R squared after leave-one-out procedure: $r^2_{\text{CV}} = (\text{SD} - \text{PRESS})/\text{SD}$, $\text{SD} = Y_{\text{actual}} - Y_{\text{mean}}$.
 $\text{PRESS} = \sum (Y_{\text{predicted}} - Y_{\text{actual}})$. For further explanation of these mathematical formulas see reference 14.

^cStandard error of prediction (cross-validated) = $(\text{PRESS}/(n - c - 1))^{1/2}$, n = number of rows, c = number of components.

^dRatio of r^2 explained to unexplained = $r^2/(1 - r^2)$.

^e $r^2_{\text{bs}} = r^2$ after bootstrapping.

^fStd Dev. column belongs with the bootstrapped r^2 .

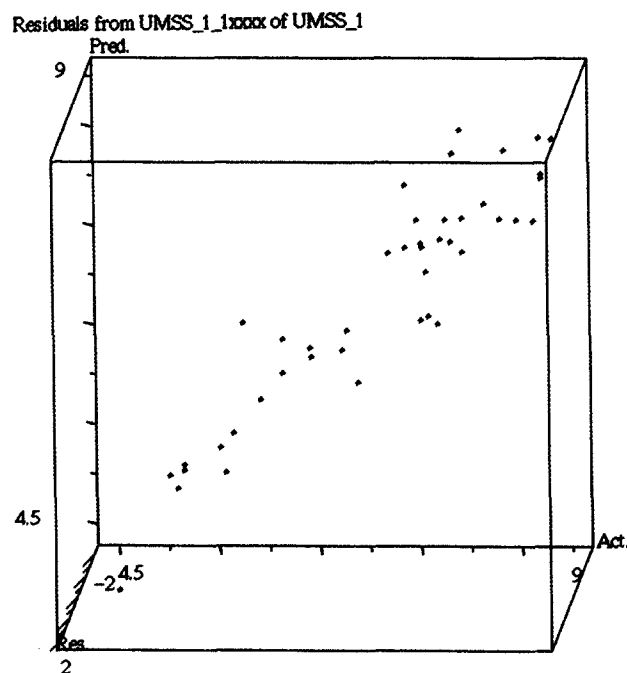


Figure 2. Predicted pK_i versus actual pK_i .

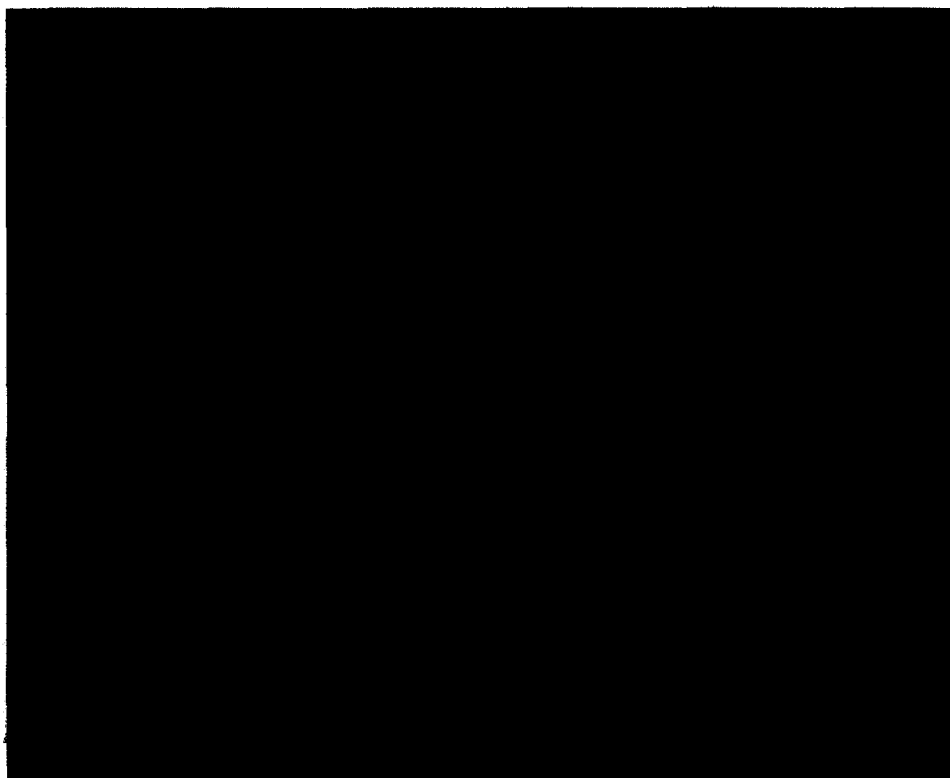


Figure 3. The CoMFA steric stdev*coeff contour plot from the analysis based on field-fit alignment. Sterically favored areas (contribution level of 80%) are represented by green polyhedra. Sterically disfavored areas (contribution level 20%) are represented by yellow polyhedra.

position of the *N*⁶-benzyl ring may not be steric but more a reflection of the importance of substitution pattern on overall stereoelectronic structure.

The binding affinities of the compounds 5–7 were predicted by CoMFA-derived QSARs. The predicted

binding affinities of these ligands (5 and 6) were comparable to the binding affinity of 26. The binding affinities of these test molecules are reported in the Table 4. The predicted binding affinity of 7 was comparable to 27. Compound 6 showed a K_i (nM) of 23, and a K_i (nM) of 47 for 7 was obtained. Comparison of actual binding



Figure 4. The CoMFA electrostatic stdev*coeff contour plot from the analysis based on field-fit alignment. Positive charges disfavored areas (contribution level 90%) are represented by blue polyhedra. Positive charge favored areas (contribution level 10%) are represented by red polyhedra.

affinity of **6** and **7** suggests a tolerance for bulky long chain groups near the 3-position of the *N*⁶-benzyl moiety. Thus, this position is suitable for derivatization by the functionalized congener approach.²⁸ The fact that compound **7** has a binding affinity similar to **27** supports the useful predictive ability of this QSAR analysis for quantifying the binding site environment of the A₃ receptor. It should be pointed out that CoMFA predicted a considerably lower binding affinity for the ligands having bulky groups at the 5'-uronamide position. Consistently, compound **17**, which also contains a Boc-NH(CH₂)₂ group, was almost inactive at A₁, A_{2a} and A₃ receptors.

On examining the predicted values (Table 4), the QSAR appears to significantly overestimate the binding affinity of the L-prolyl-substituted ligand, **5**. This suggests that a conformationally rigid bulky group causes energetically unfavorable interactions in the vicinity of the benzyl-3-position in the A₃ binding site. However, the long-chain flexible groups, such as the β-alanyl moieties, which can adjust within the binding site, are tolerated. Curiously, the rat A₁ and A_{2a} receptors did not display such strict spatial requirements in this region. The *K*_i values of the prolyl conjugate **5** at these receptors were in the 100–200 nM range. Thus, this represents a major difference in the agonist binding sites of the adenosine receptor subtypes. Identification of the amino acid residues responsible for this steric restriction in the A₃ receptor will be the subject of further studies involving both receptor molecular modeling⁵ and site-directed mutagenesis. It is to be noted that affinities of various ligands for A₃ receptors are highly species dependent, i.e. certain xanthines bind with greater affinity at sheep²⁶ and human²⁹ versus rat receptors,^{4,5} thus

the present model may be subject to modification when generalizing to other A₃ receptor clones.

Conclusion

The CoMFA method has proven to be a useful and viable means of correlating the properties of adenosine receptor ligands with biological activity, without knowing the structure of the receptor molecule. In this particular instance, the steric CoMFA map suggests that effects of bulk play a major role on binding affinity, while the electrostatic effects play a lesser role in affecting the binding affinity of the ligands. The CoMFA study has clearly shown that substituents on the 3-position of the benzyl ring affect binding affinity and selectivity for A₃ receptors by virtue of the extent of their bulkiness. We have previously shown that some bulk around the 3-position of the *N*⁶-benzyl moiety is tolerated and desirable, but our study indicates that flexible bulky groups, which can adjust inside the binding pocket, are also tolerated. Comparison of the binding affinity data of IB-MECA, **24**, and compound **7** with other ligands indicates that the binding of this class of compounds is due to hydrophobic interactions and, in addition, demonstrates the lack of an electrostatic effect. However, the A₃ affinity of ligand **7** indicates that there is a tolerance in the binding site for a sterically bulky group at the 3-position, although a less bulky hydrophobic group (e.g. iodo) is preferred.

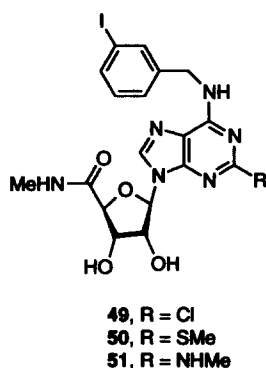
We do not have an explanation for why the prolyl-conjugate (**5**), binding affinity is not precisely predicted by CoMFA. In interpreting results of the CoMFA analysis

one must be aware of the inherent limitation that the method assumes a static receptor conformation for all ligands. Considering that possible conformational changes may occur at the binding site during ligand binding and receptor activation, the relative contributions of charge and steric interactions may not be identical for all compounds.

We performed CoMFA of compounds 49–51¹³ in a separate CoMFA training dataset (Table 2). The results suggested tolerance for steric groups at 2-position of purine ring. Thus, 2-substitution A₃ affinity-enhancing effects depend upon optimal groups at the 5'-position (5'-*N*-methyl carboxamido group) and 3-iodobenzyl group at the *N*⁶-position. Discussion of these results will be the subject of a future publication.

The CoMFA studies which we have described support the conclusion that the binding of *N*⁶-benzyladenosine-5'-uronamide derivatives is largely influenced by steric interactions of the *N*⁶-benzyl group of adenosine-5'-uronamides.

In conclusion, we have derived a working model of the A₃ adenosine receptor agonist pharmacophore using three-dimensional QSAR (CoMFA). Our model indicated that the *N*⁶-atom of the purine and the CH₂ group of benzyl moieties can be replaced by oxygen and nitrogen, respectively, without significant loss of selectivity versus A₁ and A_{2A} receptors. Our model further suggests that bulky groups at the 3-position *N*⁶-benzyl group and 2-position of purine ring (49–51) are necessary for A₃ adenosine receptor affinity. More importantly, the 3-D-QSAR model has predicted the p*K*_i values of five newly synthesized compounds (Table 4) with an accuracy comparable to that obtained by applying the cross-validation procedure in a training set of 37 analogs.



Experimental

New compounds were characterized (and resonance assigned) by 300 MHz proton nuclear magnetic resonance spectroscopy using a GEMINI-300 FT-NMR spectrometer. Unless noted, chemical shifts are expressed as ppm downfield from tetramethylsilane. Synthetic intermediates were characterized by chemical ionization mass spectrometry (NH₃) and adenosine derivatives by

fast atom bombardment mass spectrometry (positive ions in a noba or m-bullet matrix) on a JEOL SX102 mass spectrometer. In the EI mode accurate mass was determined using a VG7070F mass spectrometer. C, H, and N analyses were carried out by Atlantic Microlabs (Norcross, GA), and $\pm 0.4\%$ was acceptable. All adenosine derivatives were judged to be homogenous using thin-layer chromatography (silica, 0.25 mm, glass backed, Alltech Assoc., Deerfield, IL, U.S.A.) following final purification.

*N*⁶-[3-(*L*-Prolylamino)benzyl]adenosine-5'-*N*-methyluronamide (5). 2',3'-*O*-Isopropylidene-*N*⁶-(3-aminobenzyl)-adenosine-5'-*N*-methyluronamide (2,¹² 20 mg, 45.51 μ mol), *N*-*t*-Boc-*L*-proline (12 mg, 55.76 μ mol), *N,N'*-dicyclohexylcarbodiimide (18.77 mg, 90.98 μ mol) and imidazole (6.2 mg, 91.07 μ mol) were dissolved in anhydrous DMF. The solution was stirred at room temperature for 20 h in a sealed vessel. The solvent was evaporated by means of rotary evaporator and high vacuum. The residue was dissolved in HCl (1 M, 0.5 mL), and the resulting solution was heated to 60 °C for 40 min. After cooling in an ice bath, sodium bicarbonate solution was added to neutralize and the solvent was removed under vacuum. The residue was subjected to prep. silica gel thin layer chromatography (MeOH:CH₂Cl₂, 8:2) to give 5 as a white solid (14.2 mg, 63% yield overall). ¹H NMR (DMSO-*d*₆): δ 2.32 (*m*, 2H, CH₂), 2.70 (*d*, *J* = 4.6 Hz, 3H, CH₃), 2.73 (*m*, 2H, CH₂), 3.79 (*m*, 2H, CH₂-N), 4.2 (*m*, 1H, H-3'), 4.30 (*s*, 1H, H-4'), 4.60 (*m*, 2H, H-2'), 4.67 (*br s*, 2H, *N*⁶-CH₂Ph), 5.54 (*d*, *J* = 6.4 Hz, 1H, OH-2'), 5.70 (*d*, *J* = 4.1 Hz, 1H, OH-3'), 5.97 (*d*, *J* = 7.6 Hz, 1H, H-1'), 7.2 (*t*, *J* = 7.7, 1H), 7.40 (*d*, *J* = 7.7 Hz, 1H), 7.60 (*d*, *J* = 7.8, 1H), 7.71 (*br s*, 1H, NH-CH₂), 7.72 (*s*, 1H), 8.28 (2, 1H, H-2), 8.50 (*s*, 2H, H-8), 8.56 (*br s*, 1H, *N*⁶H-CH₂Ph), 8.80 (*br s*, 1H, NHMe) (8.90 (*br s*, 1H, NH-Ph). High resolution MS (*m/z*) measured in FAB⁺ mode: Calcd for C₂₃H₂₈N₈O₅, 496.5302, found 496.5306. Calcd for C₂₃H₂₈N₈O₅ · H₂O. Found C, H, N.

*N*⁶-[3-(β -Alanyl amino)benzyl]adenosine-5'-methyluronamide (6). 2',3'-*O*-Isopropylidene-*N*⁶-(3-aminobenzyl)-adenosine-5'-*N*-methyluronamide (2,¹² 40 mg, 91.02 μ mol), *N*-*t*-Boc- β -alanine (24 mg, 127.42 μ mol), EDAC (30 mg, 156.49 μ mol), imidazole (12.4 mg, 182.03 μ mol) and 4-dimethylaminopyridine (23 mg, 188.21 μ mol) were dissolved in anhydrous DMF. The solution was stirred at room temperature for 24 h under nitrogen. The solvent was removed *in vacuo*, and the residue dissolved in HCl (1 N, 1 mL). The resulting mixture was heated to 60 °C for 40 min. After cooling in an ice bath, conc NH₄OH was added to neutralize. The reaction mixture was loaded on a small Dowex 50X2-200 (H⁺) resin column. The column was eluted with H₂O until eluents were neutral to pH paper. Finally the column was eluted with 1 N NH₄OH, and the product-containing fractions were lyophilized to give 6 as a yellow solid (29.2 mg, 68% overall yield). ¹H NMR (DMSO-*d*₆): δ 2.63 (*m*, 2H, CH₂), 2.70 (*d*, *J* = 4.3 Hz, 3H, CH₃), 2.75 (*m*, 2H, CH₂), 4.14 (*m*, 1H, H-3'), 4.32 (*s*, 1H, H-4'), 4.59 (*dd*, *J* = 4.6 Hz, *J* = 7.5 Hz, 1H, H-2'), 4.71 (*br s*, 2H, *N*⁶-CH₂Ph), 5.55 (*d*, *J* = 6.4 Hz, 1H, OH-

2'), 5.68 (*d*, *J* = 4.1 Hz, 1H, OH-3'), 5.95 (*d*, *J* = 7.4 Hz, 1H, H-1'), 7.10 (*t*, *J* = 7.7 Hz, 1H), 7.35 (*d*, *J* = 7.7 Hz, 1H), 7.58 (*d*, *J* = 7.8, 1H), 7.72 (*s*, 1H), 8.30 (*s*, 1H, H-1), 8.44 (*s*, 1H, H-8), 8.56 (*br s*, 1H, N^6H-CH_2PH), 8.80–8.89 (*m*, 2H, $NH-Me$ and $NH-Ph$). High resolution MS (*m/z*) measured in FAB⁺ mode: Calcd for $C_{21}H_{26}N_8O_5$ 470.4919, found 470.4921. Calcd for $C_{21}H_{26}N_8O_5 \cdot H_2O$. Found C, H, N.

*N*⁶-[3-(*N*-*t*-Boc- β -alanyl amino)benzyl]adenosine-5'-methyluronamide (7). A solution of compound 6 (10 mg, 21.25 μ mol), di-*tert*-butyldicarbonate (5.5 mg, 25.2 μ mol) and triethylamine (20 μ L) in anhydrous DMF (0.5 mL) were stirred at room temperature under nitrogen. The solvent was removed *in vacuo* and the residue was purified by prep. silica gel TLC (eluent CH_2Cl_2 :MeOH, 9:1) to give 7 as white solid (9.7 mg, 80% yield overall). ¹H NMR (DMSO-*d*₆): δ 1.38 (*s*, 9H, CH_3), 2.71 (*m*, 2H, CH_2), 3.26 (*m*, 2H, CH_2), 3.31 (*d*, *J* = 4.3 Hz, 3H, CH_3), 4.12 (*m*, 1H, H-3'), 4.33 (*s*, 1H, H-4'), 4.60 (*dd*, *J* = 4.6 Hz, *J* = 7.5 Hz, 1H, H-2'), 4.70 (*br s*, 2H, N^6-CH_2PH), 5.53 (*d*, *J* = 6.4 Hz, 1H, OH-2'), 5.71 (*d*, *J* = 4.1 Hz, 1H, OH-3'), 5.60 (*d*, *J* = 7.4 Hz, 1H, H-1'), 7.13 (*t*, *J* = 7.7 Hz, 1H), 7.40 (*d*, *J* = 7.7 Hz, 1H), 7.60 (*d*, *J* = 7.8, 1H), 7.71 (*s*, 1H), 8.28 (*s*, 1H, H-1), 8.42 (*s*, 1H, H-8), 8.56 (*br s*, 1H, N^6H-CH_2PH), 8.55 (*br s*, 1H, $NH-Me$), 8.90 (*br s*, 1H, $NH-Ph$), 9.80 (*br s*, 1H, CH_2NN-CO). High resolution MS (*m/z*) measured in FAB⁺ mode: Calcd for $C_{26}H_{34}N_8O_7$ 570.6103, found 570.6106. Calcd for $C_{26}H_{34}N_8O_7 \cdot H_2O$. Found C, H, N.

6-(*N*'-Phenylhydrazinyl)purine-9- β -ribofuranoside-5'-*N*-methyluronamide (10). 2',3'-Isopropylidene-6-chloro-purine-9- β -ribofuranoside-5'-*N*-methyluronamide (1¹², 30 mg, 85.04 μ mol), phenylhydrazine (10 mg, 92.5 μ mol), and triethylamine (23.7 μ L, 0.70 mmol) were dissolved in absolute EtOH (1 mL). The solution was stirred at 70 °C for 16 h under nitrogen. The solvent was evaporated under a stream of nitrogen, and HCl (1 N, 1 mL) was added, and the resulting solution was heated to 60 °C for 40 min. After cooling in an ice bath, sodium bicarbonate solution was added to neutralize. Volatiles were removed *in vacuo* and the residue was purified by prep. silica gel TLC (eluent CH_2Cl_2 :MeOH, 8:2) to obtain 18 mg (55%) of the title compound. ¹H NMR (DMSO-*d*₆): δ 3.29 (*d*, *J* = 4.3 Hz, 3H, CH_3), 4.20 (*m*, 1H, H-3'), 4.35 (*s*, 1H, H-4'), 4.60 (*dd*, *J* = 4.6 Hz, *J* = 7.5 Hz, 1H, H-2'), 5.50 (*d*, *J* = 6.4 Hz, 1H, OH-2'), 5.68 (*d*, *J* = 4.1 Hz, 1H, OH-3'), 5.66 (*d*, *J* = 7.4 Hz, 1H, H-1'), 6.93 (*m*, 3H, Ph), 7.31 (*m*, 2H, Ph), 8.29 (*s*, 1H, H-1), 8.43 (*s*, 1H, H-8), 8.56 (*br s*, 2H, $NH-NH$), 8.55 (*br s*, 1H, $NH-Me$). High resolution MS (*m/z*) measured in FAB⁺ mode: Calcd for $C_{17}H_{19}N_7O_4$ 385.3855, found 385.38550. Calcd for $C_{17}H_{19}N_7O_4$. Found C, H, N.

6-(*O*-Phenylhydroxylamino)purine-9- β -ribofuranoside-5'-*N*-methyluronamide (11). 2',3'-*O*-Isopropylidene-6-chloro-purine-9- β -ribofuranoside-5'-*N*-methyluronamide (1, 1¹² 30 mg, 85.04 μ mol), and Dowex 30X2-200 (H⁺ resin, 2 mL, dry volume) in H₂O (3 mL) were heated at 80 °C for 1 h. The reaction mixture was made slightly basic by adding conc NH_4OH , filtered and filtrates evaporated to dryness. The residue was co-evaporated a few times with absolute EtOH. Thereafter, *O*-phenylhydroxylamine hydrochloride

(18 mg, 124.2 μ mol) and triethylamine (23.7 μ L, 0.70 mmol) were added and the resulting mixture heated at 65 °C for 24 h. The solvent was removed under a stream of nitrogen and the residue was purified by TLC (eluent CH_2Cl_2 :MeOH, 8:2) to obtain 17 mg (52%) of the title compound. ¹H NMR (DMSO-*d*₆): δ 3.26 (*d*, *J* = 4.3 Hz, 3H, CH_3), 4.22 (*m*, 1H, H-3'), 4.31 (*s*, 1H, H-4'), 4.62 (*dd*, *J* = 4.6 Hz, *J* = 7.5 Hz, 1H, H-2'), 5.53 (*d*, *J* = 6.4 Hz, 1H, OH-2'), 5.70 (*d*, *J* = 4.1 Hz, 1H, OH-3'), 5.70 (*d*, *J* = 7.4 Hz, 1H, H-1'), 6.90 (*m*, 3H, Ph), 7.30 (*m*, 2H, Ph), 8.30 (*s*, 1H, H-1), 8.41 (*s*, 1H, H-8), 8.56 (*br s*, 1H, $NH-O$), 8.55 (*br s*, 1H, $NH-Me$). High resolution MS (*m/z*) measured in FAB⁺ mode: Calcd for $C_{17}H_{18}N_6O_5$ 386.3702, found 386.3705. Calcd for $C_{17}H_{18}N_6O_5$. Found C, H, N.

Cell culture and radioligand binding

CHO cells stably expressing the A₃ receptor^{5,16} were grown in F-12 medium containing 10% FBS and penicillin/streptomycin (100 U mL⁻¹ and 100 μ g mL⁻¹ respectively) at 37 °C in a 5% CO₂ atmosphere, and membrane homogenates were prepared as reported.¹⁶

Binding of [¹²⁵I]4-amino-3-iodobenzyladenosine-5'-*N*-methyluronamide ([¹²⁵I]AB-MECA) to the CHO cells membranes was performed essentially as described.^{12,16} Assays were performed in 50:10:1 buffer in glass tubes and contained 100 μ L of the membrane suspension, 50 μ L [¹²⁵I]AB-MECA (final concentration 0.3 nM) and 50 μ L inhibitor. Inhibitors were routinely dissolved in DMSO and were then diluted with buffer; final DMSO concentrations never exceeded 1%. Incubations were carried out in duplicate for 1 h at 37 °C, and were terminated by rapid filtration over Whatman GF/B filters, using a Brandell cell harvester (Brandell, Gaithersburg, MD, U.S.A.). Tubes were washed three times with 3 mL of buffer. Radioactivity was determined in a Beckman gamma 5500B γ -counter. Non-specific binding was determined in the presence of 40 μ M R-PIA. *K*_i-values were calculated according to Cheng-Prusoff,³⁰ assuming a *K*_d for [¹²⁵I]AB-MECA of 1.55 nM.¹⁶

Binding of [³H]PIA to A₁ receptors from rat brain membranes and of [³H]CGS 21680 to A₂ receptors from rat striatal membranes was performed as described previously.^{17,18} Adenosine deaminase (3 U mL⁻¹) was present during the preparation of brain membranes, in which an incubation at 30 °C for 30 min is carried out, and during the incubation with radioligand. At least six different concentrations spanning three orders of magnitude, adjusted appropriately for the IC₅₀ of each compound, were used. IC₅₀ values, computer-generated using a non-linear regression formula on the InPlot program (GraphPAD, San Diego, CA, U.S.A.), were converted to apparent *K*_i values using *K*_d values of 1.0 and 14 nM for [³H]PIA and [³H]CGS 21680 binding, respectively, and the Cheng-Prusoff equation.³⁰

Acknowledgment

The authors would like to thank Dr X.-D. Ji and Dr N. Melman for carrying out receptor binding assays, and Dr

Gary L. Stiles and Dr Mark E. Olah (Duke University) for preparing the radioligand [¹²⁵I]AB-MECA. We would like to extend our appreciation to Dr A. M. van Rhee (NIDDK/NIH) and Dr Scott A. DePriest (Tripos, Inc.) for many valuable suggestions.

Supplementary Material Available

Coordinates of template compound **24** (IB-MECA) are available (5 pages) from the authors.

References and Notes

- Jacobson, K. A.; van Galen, P. J. M.; Williams, M. *J. Med. Chem.* **1992**, *35*, 407.
- Stiles, G. L. *J. Biol. Chem.* **1992**, *267*, 6451.
- van Galen, P. J. N.; Stiles, G. L.; Michaels, G.; Jacobson, K. A. *Med. Res. Rec.* **1992**, *12*, 423.
- Zhou, Q. Y.; Li, C. Y.; Olah, M. E.; Johnson, R. A.; Stiles, G. L.; Civelli, O. *Proc. Natl. Acad. Sci. U.S.A.* **1992**, *89*, 7432.
- van Galen, P. J. M.; van Bergen, A. H.; Gallo-Rodriguez, C.; Melman, N.; Olah, M. E.; IJzerman, A. P.; Stiles, G. L.; Jacobson, K. A. *Mol. Pharmacol.* **1994**, *45*, 1101.
- Ramkumar, V.; Stiles, G. L.; Beaven, M. A.; Ali, H. *J. Biol. Chem.* **1993**, *268*, 6887.
- Ali, H.; Cunha-Melo, J. R.; Saul, W. F.; Beavan, M. F. *J. Biol. Chem.* **1990**, *265*, 745.
- Fozard, J. R.; Carruthers, A. M. *Br. J. Pharmacol.*, **1993**, *109*, 3.
- Jacobson, K. A.; Nikodijević, O.; Shi, D.; Gallo-Rodriguez, C.; Olah, M. E.; Stiles, G. L.; Daly, J. W. *FEBS Letters* **1993**, *336*, 57.
- von Lubitz, D. K. J. E.; Lin, R. C.-S.; Popik, P.; Carter, M. F.; Jacobson, K. A. *Eur. J. Pharmacol.* **1994**, *263*, 59.
- Liu, G. S.; Richards, S. C.; Olsson, R. A.; Mullane, K.; Walsh, R. S.; Downey, J. M. *Cardiovasc. Res.* **1994**, *28*, 1057.
- Gallo-Rodriguez, C.; Ji, X.-D.; Melman, N.; Siegman, B. D.; Sanders, L. H.; Orlina, J.; Pu, Q.-L.; Olah, M. E.; van Galen, P. J. M.; Stiles, G. L.; Jacobson, K. A. *J. Med. Chem.* **1994**, *37*, 636.
- Kim, H. O.; Ji, X.-d.; Siddiqi, S. M.; Olah, M. E.; Stiles, G. L.; Jacobson, K. A. *J. Med. Chem.* **1994**, *37*, 3614.
- Cramer, R. D.; Patterson, D. E.; Bunce, J. D. *J. Am. Chem. Soc.* **1988**, *110*, 5959.
- Cramer, R. D.; Bunce, J. D.; Patterson, D. E.; Frank, I. E. *Quant. Struct.-Act. Relat.* **1988**, *7*, 18.
- Olah, M. E.; Gallo-Rodriguez, C.; Jacobson, K. A.; Stiles, G. L. *Mol. Pharmacol.* **1994**, *45*, 978.
- Schwabe, U.; Trost, T. *Naunyn-Schmiedeberg's Arch. Pharmacol.* **1980**, *313*, 179.
- Jarvis, M. F.; Schulz, R.; Hutchison, A. J.; Do, U. H.; Sills, M. A.; Williams, M. *J. Pharmacol. Exp. Ther.* **1989**, *251*, 888.
- The program SYBYL 6.04a is available from TRIPOS Associates, St. Louis, MO, U.S.A., 1993.
- MOPAC 6.0 available from the Quantum Chemistry Program Exchange.
- Dewar, M. J. S.; Zoebisch, E. G.; Haley, E. F.; Stewart, J. J. P. *J. Am. Chem. Soc.* **1985**, *107*, 3902.
- Dewar, M. J. S.; Zoebisch, E. G. *Theochem* **1988**, *49*, 1.
- Wold, S.; Ruhe, A.; Wold, H.; Dunn, W. J. *SIAM J. Sci. Stat. Comp.* **1994**, *5*, 735.
- van Galen, P. J. M.; Leusen, F. J. J.; IJzerman, A. P.; Soudijn, W. *Eur. J. Pharmacol.* **1989**, *172*, 19.
- Waller, C. L.; Oprea, T. I.; Giolitti, A.; Marshall, G. R. *J. Med. Chem.* **1993**, *36*, 4152.
- Linden, J.; Taylor, H. E.; Robeva, A. S.; Tucker, A. L.; Stehle, J. H.; Rivkees, S. A.; Fink, J. S.; Reppert, S. M. *Mol. Pharmacol.* **1993**, *44*, 524.
- Safe, S. H. *Annu. Rev. Pharmacol. Toxicol.* **1986**, *39*, 259.
- Jacobson, K. A.; Kirk, K. L.; Padgett, W. L.; Daly, J. W. *J. Med. Chem.* **1985**, *28*, 1341.
- Salvatore, C. A.; Jacobson, M. A.; Taylor, H. E.; Linden, J.; Johnson, R. G. *Proc. Natl. Acad. Sci.* **1993**, *90*, 10365.
- Cheng, Y. C.; Prusoff, W. H. *Biochem. Pharmacol.* **1973**, *22*, 3099.
- Bruns, R. F.; Lu, G. H.; Pugsley, T. A. *Mol. Pharmacol.* **1986**, *29*, 331.

(Received in U.S.A. 31 March 1995; accepted 25 May 1995)